MEASURED WINTER PERFORMANCE OF
STORM WINDOWS

J. H. Klems

Windows and Daylighting Group, Building Technologies Department
Lawrence Berkeley National Laboratory, Berkeley, California 94720-8134

Abstract

Direct comparison measurements were made between various prime/storm window combinations and a well-weatherstripped, single-hung replacement window with a low-E selective glazing. Measurements were made using an accurate outdoor calorimetric facility with the windows facing north. The double-hung prime window was made intentionally leaky. Nevertheless, heat flows due to air infiltration were found to be small, and performance of the prime/storm combinations was approximately what would be expected from calculations that neglect air infiltration. Prime/low-E storm window combinations performed very similarly to the replacement window. Interestingly, solar heat gain was not negligible, even in north-facing orientation.

Introduction

Over the past two decades there has been a great improvement in the number and performance of energy-efficient window products available in the marketplace, with the introduction of low-E and selective low-E glazings, gas-filled units, improved frames and insulating spacers. However, most of these improved products are new window units, installed in new construction or as a complete window replacement (e.g., in remodelling). They do not address the problem of inefficient windows already in place. And this is not a small problem. From existing data (U. S. Department of Energy 2002) one can estimate that 90% of the present residential building stock already existed in 1980, before development of most of the new technologies, and that around 43% of the windows in the country are still single glazed.

Window replacement (which accounts for slightly more than half of window sales) is costly, and given the notoriously high implicit discount rates of consumers, it is likely that the present replacement rate is not primarily determined by the economic payback of energy savings. Certainly, given the present spectrum of available products, it is difficult to imagine an improvement of energy efficiency in new products that would motivate a significant increase in the replacement rate. But even if one assumes that all window replacements are of single glazing, at the present rate it would take at least a decade to upgrade all of the existing single glazed windows. Retrofit products to improve the energy performance of these windows therefore promise significant near-term energy savings.

Since the introduction of "hard-coat" low-E glass it has been clear that storm window performance could be improved. If one calculates the performance of a prime/storm window combination *assuming that the unit is perfectly sealed*, one obtains a U-factor very similar to that of a sealed-insulating-glass (SIG) unit with an air fill. Typically the air gap is larger than optimal for the storm window, but on the other hand there is no spacer with its corresponding edge heat loss, and there is a double-sash framing system that is likely to have higher thermal resistance than the single-sash that holds a SIG. A gas fill, of course, is not an option for a storm window, and lower emissivities are typically available in "soft-coat" low-E glass than for "hard-coat". Theoretically, therefore, one cannot expect to equal the performance of the best new replacement window by adding a low-E storm window to an existing single-glazed window, but one can obtain a sizable fraction of the available improvement.

The problem with this calculation is that one must assume a perfectly sealed unit. Prime/storm window combinations cannot be perfectly sealed. An existing single glazed prime window is likely to be leaky—

possibly very leaky—and there are practical limits on how greatly this can be improved by weatherstripping. An exterior storm window must have a leakage rate higher than that of the prime window in order to prevent condensation. While an interior storm window can be made to have very low air leakage, it is then difficult to justify a great deal of effort in also sealing the prime window, and preventing condensation argues against sealing the prime window too well. The result is that frequently an interior storm window is used in lieu of weatherstripping the prime window at all. A reasonable assumption, therefore, is that in a prime/storm window combination there will be some exchange of the air between the glazings (gap air) with the indoor or outdoor air. This could be caused by infiltration: a net flow through both prime and storm windows that also entrains some of the gap air. But even in the absence of infiltration between interior and exterior, stack effects or local spatial variations in wind pressure could cause mixing between the gap air and the outdoors through leaks in the exterior unit. Of course, both effects could occur simultaneously. Thus, in addition to the straightforward transport of heat by any net infiltrative flow, the resultant disturbance of the gap air could alter the effective conductance of the gap. This can be expected to degrade the energy performance of the prime/storm combination, and the degree to which the theoretical performance is obtainable is correspondingly uncertain.

A calculation of the air exchange would be both difficult and unconvincing. At issue are convective flows driven by small pressure differences created both by wind and by temperature differences. Calculations in this regime would require detailed computational fluid dynamics (CFD) methods; moreover, the conditions controling the process—namely the local exterior air flow distribution and the detailed geometry of the leakage flow paths—are both time-dependent and poorly characterized in any realistic situation.

Testing under realistic outdoor conditions is needed. In 1991-2 we had conducted tests of an exterior storm window using our outdoor window test facility that indicated that air infiltration was less of a problem than might be supposed. However, we did not consider these tests conclusive because the prime window had in that case been non-operable and unrealistically well-sealed. Here we readdressed the issue by conducting tests with a realistic prime window, and we will discuss the results for winter conditions. Tests under summer conditions are still in progress.

Procedure

Tests were conducted in our accurate window thermal test facility (Klems, Selkowitz et al. 1982) at its field site in Reno, Nevada. This is a mobile facility consisting of two accurate room-sized calorimeters that expose the test sample to an outdoor environment, as shown in **Figure 1**. The calorimeters can be oriented as a pair to face any direction, and all of the information necessary to characterize window thermal performance (temperature, wind speed and direction, incident solar intensity and exterior radiant temperature) is measured on-site continuously throughout the tests. While a number of quantities are measured in the facility, the basic measurement is a continuous determination of the net energy flowing through the test sample as a function of time. Data averaged over 10-minute intervals is available. The accuracy level of the measurements has been well characterized. (Klems 1992) A tracer-gas system measures the infiltration rate in each calorimeter, and the differential air pressure across the wall holding the window in each is measured. The facility was oriented so that the windows were north-facing during these tests, in order to de-emphasize passive solar gains by preventing direct sunlight from being incident on the windows.

Figure 1. A View of the Test Facility. The faces of the two calorimeter chambers holding the test samples is shown. Left: Chamber B, holding the replacement window; Right: Chamber A with the prime/exterior storm combination. Also visible are the pyranometer and pyrgeometer (circular objects at top of wall, center) that measure the incident solar flux and sky temperature, and a portion of the weather tower (top, center) holding the wind speed and direction sensors.

Test Plan

The tests were designed to represent as directly as possible the choices available for improving an existing single-glazed window. In one of the calorimeters we mounted a single-glazed, double-hung prime window, and in the other an efficient replacement window. The latter was a purchased single-hung window with selective low-E, argon-filled sealed-insulating glazings and a well-weatherstripped vinyl frame. This "replacement window" served as a comparison for a series of tests carried out by varying the system in the other calorimeter, as listed in **Table 1**. It was intended to be reasonably representative of current practice; we selected it from a popular, high-quality line of replacement windows, and chose single-hung because this is a more usual consumer choice in this line. Other features of the particular window selection were dictated primarily by the geometric constraints of the test apparatus.

Table 1. Test Plan

Test	Dates	Sample in Calorimer Chamber	
		Chamber A	**Chamber B**
Prime Only	Jan 27-Feb 7, 2002	Prime Window alone	Replacement Window
Low-e Ext. Storm	Feb 16-20, 2002	Prime with Low-e Exterior Storm	Replacement Window
Reg. Ext. Storm	Feb 26-March 3, 2002	Prime with Uncoated Exteior Storm	Replacement Window
Low-e Int. Storm	March 13-18, 2002	Prime with Low-e Interior Storm	Replacement Window

The prime window was a custom-made, unweatherstripped, double-hung single-glazed wood window. It was intended to represent a typical candidate for retrofit. The total glass area was matched to that of the replacement window, as shown in Figure 2; the total glazed area in both windows is 0.830 m^2 (8.93 ft^2). The total area (rough opening) of each window is 1.101 m^2 (11.9 ft^2). Vertical cross-sections of the two prime/storm combinations tested are shown in Figure 3. The fit of the sashes in the frame of the prime window was adjusted in the laboratory, prior to installation at the test site, to give an air leakage rate of 40.3 m^3/hr at 75 Pa applied pressure difference (1.4 CFM/lftc at 0.3 inch H$_2$O). This corresponds to a
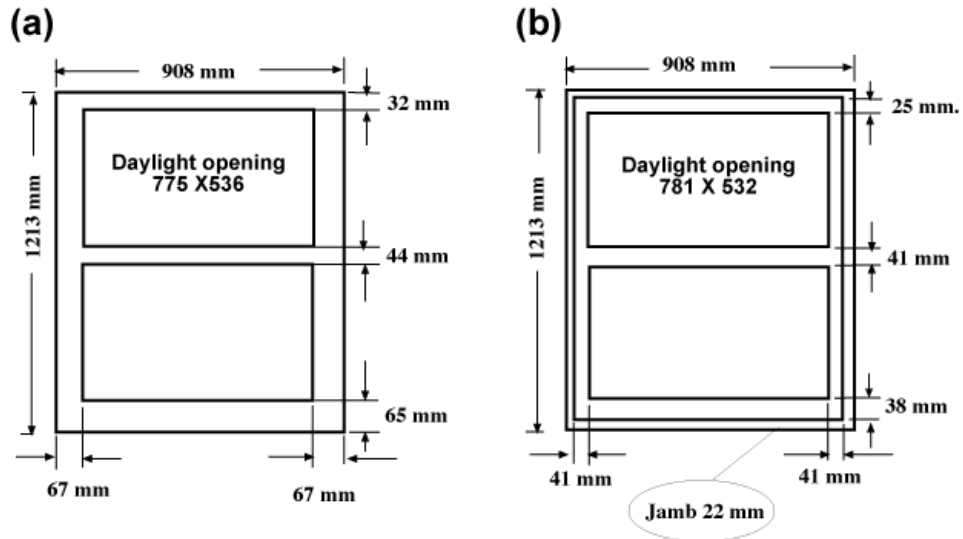
Figure 2. Tested Window Units. (a) Replacement Window. (b) Prime Window.
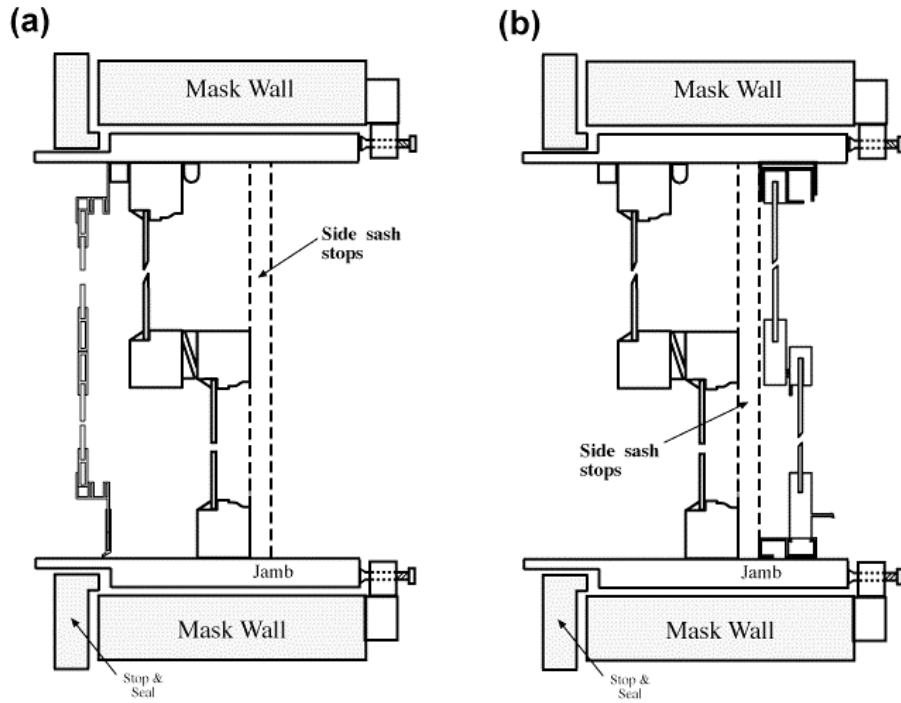
Figure 3. Cross Sections of the Prime/Storm Window Combinations Tested. (a) Exterior Storm Window. (b) Interior Storm Window.

leakage area of 11.9 cm^2 at 4 Pa (0.11 in^2/lftc at 0.3 inch H$_2$O), which is close to the "best estimate" value for an unweatherstripped double-hung window listed in the 1997 ASHRAE Handbook (ASHRAE 1997). Of course, existing windows are known to have a wide distribution of air leakage rates (Tamura 1975; Weldt and Selkowitz 1981), and some of them may be very leaky indeed (Desjarlais, Childs et al. 1998). Clearly it makes no sense to test a window with an unrealistically large leakage—one could surely make a storm window irrelevant by choosing a sufficiently large leakage. On the other hand, too low a leakage would give the opposite bias to the measurement. We reasoned that the "best estimate" value is a fair choice. A window with this leakage rate might plausibly have a storm window added without weatherstipping (although this is not the recommended procedure), or this value might result from modest weatherstripping of a much leakier older window. Any prime window that could not achieve this value through weatherstipping would probably be a candidate for replacement in any case, because of warping, decay, etc.

Preliminaries

Before the start of the tests a calorimeter chamber intercomparison was made by running for a time (on the order of a week) with identical frameless, clear double-glazed SIG units as samples. The results of this test are discussed below. Air leakage pressurization tests on both the prime and replacement windows were conducted both in the laboratory and in-situ after installation in the calorimeters. Another in-situ pressurization test was made on each prime/storm window combination prior to beginning its test run.

Data Selection

Each test was run for a considerably longer period than shown in **Table 1**. Data from these periods were selected for use in **Table 1** according to several criteria. First, since the weather patterns varied considerably during some of the tests, a period of consistently cold (nighttime) conditions was selected where possible. To the extent possible from the available data, periods of precipitation were excluded, since we cannot adequately determine all of the physical variables necessary to account for latent heat transfer to precipitation adsorbed on the exterior glass. Finally, data was selected to avoid periods, insofar as possible, when there were equipment malfunctions. The electronic equipment of the facility, especially the temperature controllers, occasionally show a transient malfunction, or "glitch". There has been an ongoing effort to diagnose and eliminate or reduce the frequency of these glitches, but this has not yet been wholly successful. Glitches appear to be random and unrelated to the conditions in the calorimeters, stemming apparently from electronic noise or power line transients. During the course of the tests, for example, the Chamber A temperature controller was replaced with a new unit with better noise immunity, and this improved performance considerably. With the exception of the temperature controllers, the normal result of a glitch is that a particular measurement (e.g., a temperature) will be nonsense for one (10-minute) data point; this is easily recognizable, and the datum (or, if necessary, all measurements) for that time can be discarded. However, when noise occurs in the control sensor input of one of the temperature controllers (or elsewhere in the controller) the result is that the HVAC system is misadjusted, causing the calorimeter temperature to depart from its setpoint. Even a small deviation from the setpoint temperature causes transient heat flows due to thermal storage in the calorimeter, resulting in a change in the apparent heat flow through the sample. Although to a certain extent we could make corrections for this effect, in these tests we chose select the data to avoid these transients where possible.

Results

The results from test of the prime window alone are shown in **Figure 4**. The most important determinants of the window heat flows are the wind speed and outdoor temperature, shown in parts (a) and (b) of the figure, respectively. Wind speed is relevant because of the potential importance of
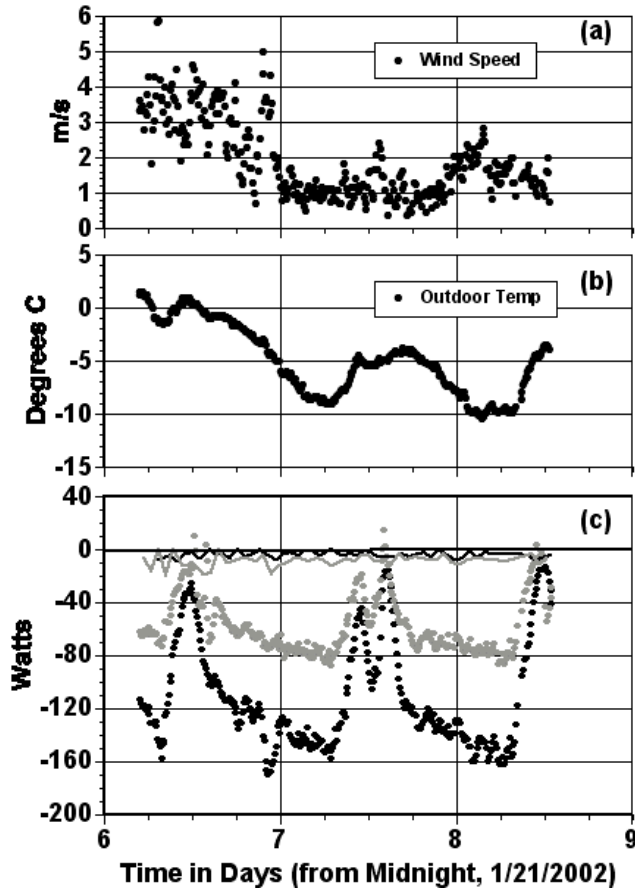
Figure 4. Prime-Only Test Results. (a) Wind speed during the tests as measured on-site at 10m height. (b) Outdoor air temperature. (c) Sample and infiltrative heat flows: Black points: Net heat flow through the prime window, measured at 10-min intervals; gray points: net heat flow through the replacement window; black curve: heat flow due to infiltration through the prime window; gray curve: heat flow due to infiltration through the replacement window. Negative heat flow represents a heat loss from the interior space.

infiltration. The interior air temperatures of the the two calorimeter chambers are kept essentially constant—within a few tenths of a degree of 20 ºC (68 ºF). Not shown are the incident solar energy and the sky temperature; both of these affect the window heat flows, but will not directly figure into the discussion. The key measured quantities are the net heat flows shown as collections of points in part (c) of the figure. Each point represents a separate, independent measurement of the net heat flow through the window (and adjacent mask wall) in question, black points indicating measurements on the prime window (mounted in calorimeter Chamber A) and gray indicating the replacement window (Chamber B). Taken together, these points trace out a curve representing the heat flow through the window as a function of time. These measurements represent the "base case" of the prime window before improvement by the addition of a storm window.

It can be seen from the two net heat flow curves that the prime window has approximately twice the rate of heat loss of the replacement window at nighttime. During the day one sees peaks due to solar heat gain, even though in a north-facing orientation only diffuse solar flux is incident. As a result, there is considerably less difference in the daytime net heat flow through the respective windows than in the nighttime. One sees from this why it is important to be able to measure the net heat flow on a short time scale, rather than the average over a longer period such as a day, if one is to understand the details of the differences in performance.

The net heat flow is determined by combining measurements of the heat flows or changes in heat content of all the elements of the calorimeter except the region designated as the "sample":

- Changes in the heat content of the calorimeter air and adjacent materials
- Heat added to the calorimeter air by heaters, fans and internal equipment
- Heat removed from the calorimeter by the HVAC cooling system
- Heat flowing into the chamber air from the materials of the calorimeter shell

The first term is kept negligibly small by keeping the calorimeter air temperature constant; energy is added by electrical heaters, fans, etc, which are monitored by accurate wattmeters; removed heat is measured by measuring the flow rate and temperature rise of the coolant; and heat exchange with the calorimeter shell is measured by a set of custom large-area heat flow sensors.(Klems, Selkowitz et al. 1982) The "sample" is the part of the calorimeter shell not covered by the large-area heat flow sensors.

6

This consists of the window and the immediately surrounding "mask" wall. The measured net heat flow is thus the sum of the heat flow through the window and the mask wall. (The latter is termed the "flanking heat flow".) Since the flanking heat flow is the same for both calorimeters (a point discussed later), differences in net heat flow are due to differences in the heat flow through the respective windows. For this reason the tests were structured as a direct comparison between the system of interest and a constant control, the replacement window.

Infiltration Heat Flow

Also shown in **Figure 4(c)** are two continuous curves representing the infiltration heat flow Q_{INF} through the two samples. These were inferred from the measured rates of change in concentration of a tracer gas in each calorimeter and the differences in temperature between the interior and exterior air:

$$Q_{INF} = \rho C_P \frac{dV}{dt}\left(T_{out} - T_{in}\right) \qquad (1)$$

where,

    ρ is the density of air

    C_P is the specific heat of air

    $\dfrac{dV}{dt}$ is the volumetric infiltration rate (inferred from changes in the tracer gas concentration)

    T_{out}, T_{in} are the exterior and interior air temperatures, respectively.

Infiltration flow is caused by pressure differences between the interior and exterior air, and requires (at least) two leakage paths, one of which infiltrates while the other exfiltrates. The heat flow in Equation (1) becomes observable because of the entry of unconditioned air in the infiltration part of the process; in order to maintain a constant interior temperature, the HVAC system must condition this air, either by adding heat (winter) or removing heat (summer). (Changes in moisture content must also be accounted for, but they are irrelevant in these tests, since (a) the humidity level was not controlled, and (b) humidity in Reno is low.) In a normal building situation both leaks are to the out-of-doors; in the calorimeters, however, the shells have negligible leakage, and other than through the sample the only leakage is a small and well-characterized leak through a pipe to the equipment room, which is at approximately the same temperature as the calorimeter chamber. Therefore, when infiltration is through the sample and exfiltration is through the calorimeter/equipment room leak, the calorimeter will record a net heat flow, but there will be no heat flow for the reverse process. For the thermally driven stack effect, there will be infiltration through one part of the sample and exfiltration through another, and Equation 1 will apply. The pressure differences across parts of the sample generated by the stack effect will be of the order of 0.5-1.4 Pa (0.002-0.006 inches H_2O).

It is therefore necessary to address the question of pressure differences across the sample. In addition to a tracer-gas measurement system, each calorimeter was instrumented with differential pressure sensors measuring the difference between the pressure at the mid-height of the sample face and the interior pressure of the calorimeter chamber. The measurements are again 10-minute averages. Measurements for the prime window for a period before and including the data of **Figure 4** are shown in **Figure 5**. The data in this figure include the highest peak wind speed measured in all of the tests. **Figure 5(a)** shows a pattern similar to what one would expect: at low wind speeds the pressure differences are in the range expected for stack effects, and are relatively insensitive to wind speed; at higher wind speeds (above 2 m/s (4.2 MPH)) one observes larger pressure differences, presumably those induced by the wind. **Figure 5(b)**, however, shows that the correlation of the pressure differences with the wind velocity (as measured at the weather tower) is not particularly strong. Even when one restricts attention to cases where the wind
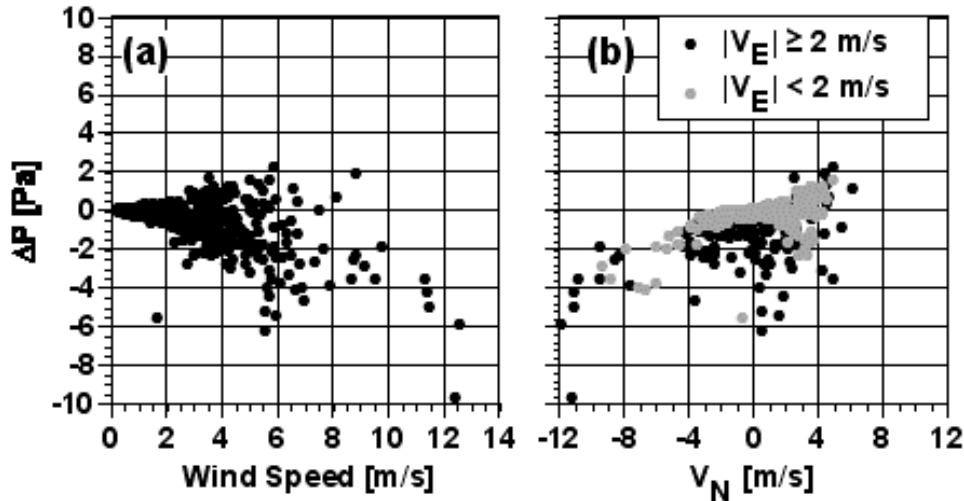
is strongly either windward or leeward with respect to the window (gray points in the figure) a clear

Figure 5. Relationship Between Wind Velocity and Pressure Difference Across Prime Window. (a) Pressure difference vs wind speed. (b) Wind speed and direction have been combined to produce wind velocity components along North and East axes, V_N and V_E. Positive V_N (V_E) means wind is from the north (east). Pressure difference for a given value of V_N is separately plotted for small (gray points) and larger (black points) values of V_E.

correlation with wind speed only begins to emerge at wind speeds greater than 4 m/s (8.3 MPH)—and data for these wind speeds is sparse. Negative pressure differences (window exfiltrating) appear much more common than positive, and the largest wind speeds are for southerly winds, which induce a negative pressure difference.

Two assumptions are possible for interpreting the measured infiltration rate as an infiltrative heat flow. In the first, Equation 1 is applied to all infiltration measurements, essentially assuming that all infiltration flows in through the window and out through the calorimeter/equipment room leak. This is surely an overestimate, and we term this quantity the "maximum" infiltration heat flow. (For technical reasons, infiltration measurements are only available on half-hour intervals, so half-hour averages are used in Equation 1). The second assumption, which we term the "estimated" infiltration heat flow, uses Equation 1 whenever the pressure difference is greater than –1.4 Pa (-.006 inches H_2O), but for negative pressure differences of larger magnitude assumes that wind pressure has overwhelmed the stack effect, and the window is exfiltrating; hence there is no corresponding infiltrative heat flow.

The solid curves in **Figure 4(c)** give the estimated infiltration heat flow through the two samples. It can be seen that, except at around noon, it is a small part of the net heat flowing through the two samples. This is generally true, as shown in **Table 2**. There the infiltration heat flow calculated by both methods is averaged over the entire test period and compared to the corresponding sample heat flow, similarly averaged. This heat flow is never more than 20% of the total and is generally below 10%. Whether one uses estimated or maximum infiltration heat flow does not make a great deal of difference.

Table 2. Mean Infiltration Heat Flow as Percentage of Mean Sample Heat Flow

Test	Mean wind speed	Chamber A			Chamber B		
		Mean Sample Heat Flow	Infiltration		Mean Sample Heat Flow	Infiltration	
	m/s	Watts	Est.	Max.	Watts	Est.	Max.
Prime Only	1.9	-113	8%	8%	-58	7%	7%
Low-e Ext. Storm	2.7	-34	9%	11%	-30	8%	9%
Reg. Ext. Storm	2.3	-54	7%	7%	-42	8%	9%
Low-e Int. Storm	2.8	-42	16%	17%	-43	10%	11%

Storm Window Performance

The measured comparisons between the prime/storm window combinations listed in **Table 1** and the replacement window are shown in the three parts of **Figure 6,** where each part of the figure shows a separate test. The two prime/low-E storm window combinations (**Figure 6(a)** and **6(c)**) give a net energy flow that is essentially indistinguishable from that of the replacement window. The uncoated
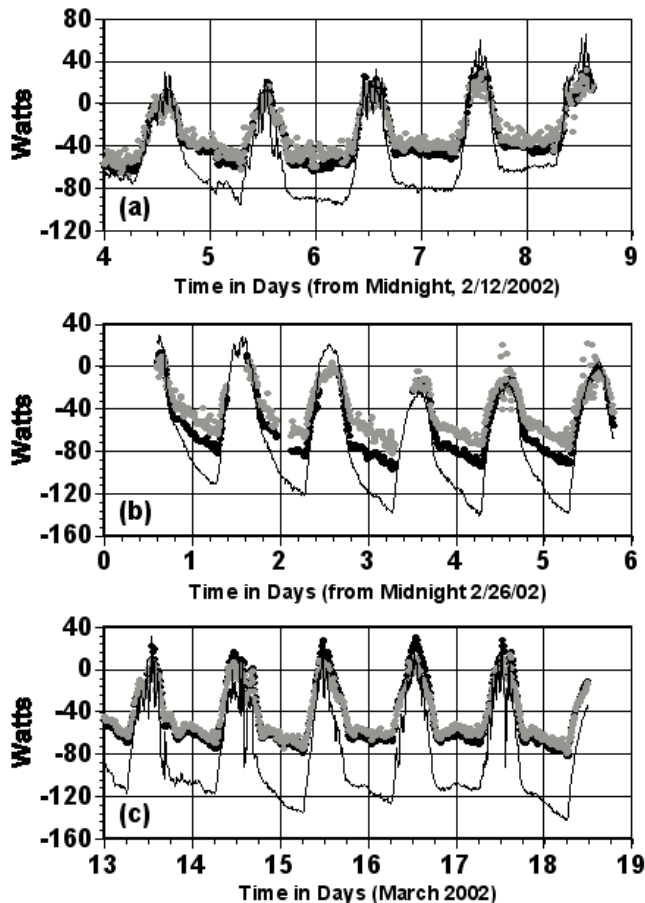
Figure 6. Performance of Prime/Storm Window Combinations. In each plot, the measured net heat flow through a prime/storm window combination (black dots) is compared with the simultaneously-measured net heat flow through the replacement window (gray dots). In addition, a continuous curve describes the calculated net heat flow though the prime window alone under the same instantaneous conditions. (a) Exterior low-e storm window tests. (b) Exterior uncoated storm window test. (c) Interior low-e storm window test.

storm window (**Figure 6(b)**) gives somewhat poorer performance, as one would expect. Note that these measurements would contain the effects of infiltration. We have shown above that the infiltration heat flow is small; here we see there are no other effects that degrade the performance of the prime/storm combinations. The calculated curve in each figure gives the net heat flow that would be expected for the prime window alone, allowing one to see the level of improvement in performance that is achieved by the addition of the storm window.

The comparisons can be made more accurate and systematic by extracting phenomenological U-factors and solar heat gain coefficients from fits of a simple model to the data. One represents the sample heat flow, W, as

$$W(t) = A \cdot \left[U \cdot \left(T_{out}(t) - T_{in}(t) \right) + g \cdot S(t) \right] \qquad (2)$$

where

A is the window area (rough opening)

U is the U-factor, a constant

g is the solar heat gain coefficient, a constant

S is the incident solar flux (here, diffuse)

t is the time

The quantities $T_{out}(t)$, $T_{in}(t)$ and $S(t)$ are all directly measured during the test, and of course A is known. The net heat flow from each test is then fit to Equation 2 and the best-fit values of U and g determined. These are listed in **Table 3**. The separate U-values obtained for the replacement window are all consistent within the quoted error. There are small statistically significant differences in the g values obtained for different measurements on this window, but this is reasonable because g depends on the angular distribution of the incident radiation, which may change with sky conditions in the separate tests. The calculation of the prime-window-only curves in **Figure 6** was made by using the U and g values for the prime window in Equation 2.

Table 3. Fitted Values of U-Factor and Solar Heat Gain Coefficient

Test	Prime or Prime/Storm Combination		Replacement Window	
	U-factor (W/m²K)	Solar Heat Gain Coefficient	U-factor (W/m²K)	Solar Heat Gain Coefficient
Prime Only	4.72±0.04	0.535±0.017	2.45±0.03	0.309±0.012
Low-e Ext. Storm	3.04±0.02	0.360±0.006	2.53±0.02	0.280±0.005
Reg. Ext. Storm	3.32±0.01	0.311±0.004	2.50±0.01	0.221±0.005
Low-e Int. Storm	2.67±0.02	0.394±0.007	2.47±0.01	0.288±0.004

Discussion

Experimental Biases

We considered a number of possible experimental biases. The chief experimental bias that would affect the conclusions of this study would be a difference in the measurement between the two calorimeter chambers, either because of miscalibration or a difference in flanking heat flow (which is included in the measured sample heat flow). As noted above, we tested for this by an initial test in which identical uncoated double-glazed SIG units were mounted in both chambers. We evaluated this test by fitting Equation 2 to the test results and obtaining values U_A and U_B for the two chambers, A and B (where Chamber A is the one used for the prime/storm combination). We did find a small, statistically significant difference, $\left(U_B - U_A \right) = -0.21 \pm 0.04 \quad \mathrm{W}/\mathrm{m}^2\,\mathrm{K}$. However, this would imply that the performance measured in Chamber A is systematically slightly worse relative to Chamber B than is true, i.e.; the measured U-value for all the prime and prime/storm combinations should be corrected downward by around 0.21. This correction, if made, would only strengthen the conclusions of **Table 3**, and in any case, the magnitude of the correction is not large. We have chosen not to make it.

This difference is not due to a difference in flanking heat flow between the two chambers. A separate test specifically designed to measure the flanking heat loss showed that differences in flanking heat flow are less than 0.01 W/m^{2}K (one standard deviation).

Table 4 lists the corrections to the measurements due to infiltration, and the resulting corrected U-factors. The infiltration corrections are based on the estimated infiltration, and as described above there is considerable uncertainty about how to assign a heat flow to the measured infiltration rates, above and beyond the quoted error in the table. The infiltration corrections are probably overestimates. The value in **Table 4** for the measured U of the replacement window is the weighted average of the measurements in **Table 3**. The fitted U-factors provide a more sensitive comparison between the windows than is easily made directly from **Figure 6**. When one compares the values in either the measured or corrected column of **Table 4**, a recognizable pattern emerges: the addition of either low-E storm produces a combination that has performance close to, but not quite as good as, that of the replacement window. This is to be expected, since the coating in the replacement window has a lower emissivity than that of the storm windows, and also the SIG is argon filled. The addition of the uncoated storm window provides a smaller performance improvement. We have not yet determined the reason that the prime/interior low-E storm window U-factor is lower than that for the prime/exterior low-E window.

Table 4. Infiltration Corrections to Measured U-Factors

Window	Measured U (W/m^{2}K)	Infiltration Correction (W/m^{2}K)	Corrected U (W/m^{2}K)
Replacement Window	2.49±0.04	0.16±.02	2.33±0.04
Prime Window	4.72±0.04	0.31±.04	4.41±0.06
Prime + Low-e Exterior Storm Window	3.04±0.02	0.20±0.02	2.84±0.03
Prime + Uncoated Exterior Storm Window	3.32±0.01	0.20±0.02	3.12±0.02
Prime + Low-e Interior Storm Window	2.67±0.02	0.29±0.04	2.38±0.05

The values listed in **Table 3** should not be confused with quantities that would be calculated using the NFRC methodology (NFRC 1993; NFRC 1994) (e.g., the program WINDOW (Windows and Daylighting Group 1994)). In addition to containing the flanking heat flows, **Tables 3** and **4** contain values that implicitly include averages over the exterior conditions occurring during the tests. The most relevant of these are the sky temperature and the air motion near the exterior window surface, both of which affect the heat transfer to the exterior glass from the surroundings. It is difficult to simulate these effects adequately in a calculation; this is another reason why a direct empirical comparison to a "base case" window is a useful procedure.

We also considered the possibility that the selection of the data period has biased the conclusions about infiltration. This might occur if the selection of data for presentation had excluded windy periods that would have higher levels of infiltration. This was particularly of concern because the selection had been (among other things) for cold exterior temperatures. In Reno these occur preferentially under clear conditions, while high winds are frequently associated with cloudy conditions (storm fronts). With this in mind, we re-examined the entire set of data collected for each test, in comparison with that selected for analysis. We found that for the exterior storm window tests (both low-E and uncoated) the selected data in fact included the windiest periods observed in those tests. The windiest period observed in any of the tests occurred during the interior storm window tests and in fact partially overlapped the selected data period. When we compared this windiest period with the "best data" period contained in **Table 1**, we found that it had a mean wind speed of 7.1 m/s (15 MPH) and a peak speed of 10.5 m/s (22 MPH) compared with 2.8 m/s (6 MPH) and 8.5 m/s (18 MPH), respectively, for the "best data" period. We analyzed the windiest period and found that the fitted values of U and g obtained were consistent with those in **Table 3**. The estimated infiltration heat flow for this period was in fact smaller than that for the "best data" period, -4 W as compared with –7W.

The highest peak wind speed observed during any of the tests, 12.7 m/s (27 MPH) occurred during the Prime Only tests on January 26, just before the "best data" period in **Table 1**. Again, there was a windy period that partially overlapped the "best data" period. When we re-examined the data, we found that January 26 had been excluded because the temperature controller in Chamber B was malfunctioning; the infiltration data and the Chamber A heat flow data were usable, however. We re-analyzed the Chamber A (prime window only) data for this period and found that again the estimated infiltration heat flow was on the average lower than for the "best data" period. A fit to the data did result in a higher U value than that in **Table 3**, but the reason was unrelated to infiltration. The 24-hour period of January 26 was an unusually clear one, and the sky temperature was low during that time; both windows show an enhanced heat transfer that is not adequately accounted for with the simple model of Equation 2.

Interpretation of Infiltration Results

A significant qualification to the infiltration results for the interior storm window must be made. The installation during the testing departed from the manufacturer's recommended practice, in that double-stick tape supplied with the unit, and intended to seal the interior storm window frame to the window jamb, was not applied. Had this been used, the measured infiltration rates may have been considerably lower. The tape was not applied because it would have prevented subsequent removal and reuse of the storm window. We already knew from the exterior storm window tests that infiltration was not a dominant effect, and therefore extra sealing of the storm window would not greatly affect the net heat flow.

A similar qualification is in order for the replacement window. This unit was very well weatherstripped and had a very low leakage rate, as our laboratory test showed. However, the in-situ tests showed a significantly higher leakage rate, apparently due to weathering of the seals that hold the test windows in

the mask wall of the facility (see **Figure 2**). This is not necessarily atypical of an actual installation, since it is well-known that leakage through the joint between window and wall is a common problem. (Weldt and Selkowitz 1981) In any case, since the resulting infiltration heat flow was low, this did not significantly affect the result. Approximately half of the infiltration correction listed in **Table 4** for the replacement window is due to leakage in the installation.

The fact that infiltration heat flows are typically small relative to window heat flows has been noted before. (Klems 1983) This work provides direct empirical verification of that study, which was a calculation based on whole-building measurements. The reason that infiltration heat flows are relatively small is worth reiterating: The standard air leakage test used for a window represents an extreme condition: a window continuously exposed to a static pressure difference of 75 Pa (0.3 inches H_2O), which is equal to the stagnation pressure of a 12 m/s (25 MPH) wind. But windows in low-rise residential buildings do not experience anything like these pressure differences, due to variation of wind speed with height, wind shielding, and the variability of both wind speed and direction. For example, **Figure 5** shows two points for which the wind speed is about 12.5 m/s (26 MPH). The logic of the static leakage test would lead one to expect a corresponding pressure difference of 81 Pa (0.33 inches H_2O). In fact the figure shows that the pressure differences actually experienced by the window were 6 Pa (0.024 inches H_2O) and 10 Pa (0.04 inches H_2O), about ten times lower than expected. In both cases the window was leeward of the wind. If we look at the point with the highest windward velocity component (and a small transverse component), the right-most gray point in **Figure 5(b)**, we find that a north component of about 5 m/s (10 MPH) corresponds to a pressure difference of about 1.5 Pa (0.006 inches H_2O). But the stagnation pressure of a 5 m/s wind would be 13 Pa (0.05 inches H_2O), again nearly ten times that observed.

When there was occasion for someone to enter the test chamber while the windows were set up for testing, the flow due to infiltration was quite perceptible. This was especially true during the March testing of the interior storm window. One can infer from this that user perception and comfort issues due to infiltration become important while the overall heat flow due to infiltration is quite small. This may explain the stringency of the standard test (although the requirements for high-rise buildings are also relevant).

The test configuration does not constitute a recommendation that prime windows not be weatherstripped. In any storm window installation, first weatherstripping the prime window as well as possible is highly recommended, with the proviso that where an interior storm window is being applied, the prime window should not sealed more tightly than the storm. (This should not be a problem with a well-designed interior storm window.)

Solar Heat Gain

One does not typically consider solar gain for north-facing windows in the wintertime, but the daytime peaks in **Figures 4** and **6** make it obvious that even though the incident solar flux is wholly diffuse, the resulting heat gain is not negligible. As one can see by comparing **Figures 4(b)** and **4(c)**, the exterior air temperature does rise during the day, but it does not by itself explain the peaks. We can separate the solar and thermal effects by using Equation 2 with the value of U obtained from the fit to the data and g set equal to zero. This gives the thermal part of the heat flow, and one can then get the solar part by subtracting this from the measured heat flow. In **Table 5** we show the average values of these quantities (expressed as heat flows) for each of the four tests. The averaging is done using the "best data" sets listed in **Table 1**, except that the averaging is restricted to integral 24-hour periods; partial days are excluded. One can see from the table that even in this north-facing orientation, solar gains account for 15-30% of the heat flow that would occur without it. (For definiteness—because the two heat flows have opposite sign—the solar fraction is defined as the ratio of the solar to the magnitude of the thermal heat flow).

Since (cf. **Table 3**) the solar heat gain coefficient differs considerably between the replacement window and the prime/storm combinations, comparison of performance is more complicated than straightforward comparison of U-factors (higher g partially compensates for higher U).

Table 5. Thermal and Solar Heat Flows During Tests

Test	Prime or Prime/Storm			Replacement Window		
	Thermal Watts	Solar Watts	Solar Fraction	Thermal Watts	Solar Watts	Solar Fraction
Prime Only	-138.6	26.0	19%	-72.0	14.1	20%
Low-e Ext. Storm	-47.5	13.5	28%	-40.4	10.5	26%
Reg. Ext. Storm	-69.3	10.2	15%	-52.1	7.1	14%
Low-e Int. Storm	-61.6	19.6	32%	-56.9	14.3	25%

Conclusions

In tests under actual winter weather conditions of north-facing prime/storm window combinations in comparison with a selective low-E replacement window, we find that

- Infiltration does not significantly degrade the expected performance. This was true even though the prime window was intentionally made moderately leaky, and (in one case) no special effort was made to seal the (interior) storm window. It would certainly be true if the interior member of the prime/storm combination were properly weatherstripped.

- The general performance pattern followed that expected from calculations made neglecting infiltration, although direct quantitative comparisons between the measurements and calculations have not yet been completed (due to the difficulty of determining exterior convective conditions).

- The addition of low-E storm windows to the prime window provided performance very similar to that of the replacement window, and expected differences in performance were only detectable through a sensitive fitting procedure (essentially, a long-term averaging).

- Solar heat gain was not negligible, even though only diffuse solar energy was incident on the windows.

Acknowledgments

References

ASHRAE (1997). 1997 ASHRAE Fundamentals Handbook. Atlanta, GA, American Society of Heating, Refrigeration and Air Conditioning Engineers**:** 29.9.

Desjarlais, A. O., K. W. Childs, et al. (1998). To Storm or Not to Storm: Measurement Method to Quantify Impact of Exterior Envelope Airtightness on Energy Usage Prior to Construction. ASHRAE/DOE/BTECC Conference on the Thermal Performance of the Exterior Envelopes of Building VII, Clearwater Beach, FL, American Society of Heating, Refrigeration and Air Conditioning Engineers (ASHRAE).

Klems, J. H. (1983). "Methods of Estimating Air Infiltration throught Windows." Energy and Buildings **5**: 243-252.

Klems, J. H. (1992). "Method of Measuring Nighttime U-Values Using the Mobile Window Thermal Test (MoWiTT) Facility." ASHRAE Trans. **98**(Pt. II): 619-29.

Klems, J. H., S. Selkowitz, et al. (1982). A Mobile Facility for Measuring Net Energy Performance of Windows and Skylights. Proceedings of the CIB W67 Third International Symposium on Energy Conservation in the Built Environment. Dublin, Ireland, An Foras Forbartha. **III:** 3.1.

NFRC (1993). NFRC 200-93: Procedure for Determining Fenestration Product Solar Heat Gain Coefficients at Normal Incidence, National Fenestration Ratings Council, Silver Spring, MD 20910.

NFRC (1994). NFRC 300-94: Procedures for Determining Solar Optical Properties of Simple Fenestration Products, National Fenestration Rating Council, Silver Spring, MD 20910.

Tamura, G. T. (1975). "Measurement of Air Leakage Characteristics of House Enclosures." ASHRAE Trans. **81**(1): 202-211.

U. S. Department of Energy (2002). Buildings Energy Databook.

Weldt, J. L. and S. Selkowitz (1981). "Field Air Leakage of Newly Installed Residential Windows." ASHRAE Trans. **85**(1): 149-159.

Windows and Daylighting Group (1994). WINDOW 4.1: A PC PRogram for Analyzing Window Thermal Performance in Accordance with Standard NFRC Procedures, Lawrence Berkeley Laboratory, Berkeley, CA 94720.